Magnetic Resonance Imaging 44 (2017) 46–54

Contents lists available at ScienceDirect

Magnetic Resonance Imaging

journal homepage: www.mrijournal.com

Original contribution

4D cardiac imaging at clinical 3.0 T provides accurate assessment of murine myocardial function and viability

Lindsey A. Crowe [a,*], Fabrizio Montecucco [b,c], Federico Carbone [b], Iris Friedli [a], Anne-Lise Hachulla [a], Vincent Braunersreuther [d], François Mach [e], Jean-Paul Vallée [a]

[a] Division of Radiology, Department of Radiology and Medical Informatics, Geneva University Hospital and Faculty of Medicine, University of Geneva, 4 rue Gabrielle-Perret-Gentil, 1205 Geneva, Switzerland
[b] First Clinic of Internal Medicine, Department of Internal Medicine, University of Genoa, 6 viale Benedetto XV, 16132 Genoa, Italy
[c] IRCCS AOU San Martino - IST, Genova, 10 Largo Rosanna Benzi, 16132 Genoa, Italy
[d] Division of Pathology, Department of Genetics and Laboratory Medicine, Geneva University Hospitals, 4 rue Gabrielle-Perret-Gentil, 1205 Geneva, Switzerland
[e] Division of Cardiology, Foundation for Medical Researches, Faculty of Medicine, Department of Internal Medicine, University of Geneva, 64 avenue de la Roseraie, 1211 Geneva, Switzerland

ARTICLE INFO

Article history:
Received 6 March 2017
Received in revised form 22 July 2017
Accepted 23 July 2017

Keywords:
4D cine
Mouse
Infarct
3 T MRI
Right ventricle

ABSTRACT

Objectives: We validate a 4D strategy tailored for 3 T clinical systems to simultaneously quantify function and infarct size in wild type mice after ischemia/reperfusion, with improved spatial and temporal resolution by comparison to previous published protocols using clinical field MRI systems.
Methods: C57BL/6J mice underwent 60 min ischemia/reperfusion (n = 14) or were controls without surgery (n = 6). Twenty-four hours after surgery mice were imaged with gadolinium injection and sacrificed for post-mortem MRI and histology with serum also taken for Troponin I levels. The double ECG- and respiratory-triggered 3D FLASH (Fast Low Angle Shot) gradient echo (GRE) cine sequence had an acquired isotropic resolution of 344 μm, TR/TE of 7.8/2.9 ms and acquisition time 25–35 min. The conventional 2D FLASH cine sequence had the same in-plane resolution of 344 μm, 1 mm slice thickness and TR/TE 11/5.4 ms for an acquisition time of 20–25 min plus 5 min for planning. Left ventricle (LV) and right ventricle (RV) volumes were measured and functional parameters compared 2D to 3D, left to right and for inter and intra observer reproducibility. MRI infarct volume was compared to histology.
Results: For the function evaluation, the 3D cine outperformed 2D cine for spatial and temporal resolution. Protocol time for the two methods was equivalent (25–35 min). Flow artifacts were reduced ($p = 0.008$) and *epi*/*endo*-cardial delineation showed good intra and interobserver reproducibility. Paired *t*-test comparing ejection volume left to right showed no significant difference for 3D ($p = 0.37$), nor 2D ($p = 0.30$) and correlation slopes of left to right EV were 1.17 ($R^2 = 0.75$) for 2D and 1.05 ($R^2 = 0.50$) for 3D.
Quantifiable 'late gadolinium enhancement' infarct volume was seen only with the 3D cine and correlated to histology ($R^2 = 0.89$). Left ejection fraction and MRI-measured infarct volume correlated ($R^2 > 0.3$).
Conclusions: The 4D strategy, with contrast injection, was validated in mice for function and infarct quantification from a single scan with minimal slice planning.

1. Introduction

Experimental cardiac MRI is important, but often difficult to perform due to the lack of small animal systems, particularly in the clinical environment. An efficient way to override this limitation is to use more widely available clinical MRI systems. Small animal imaging on clinical 3 T machines is therefore an important and cost effective step. For the validation and testing of new contrast media, results obtained at higher field may not be representative of the clinical scanner conditions when transferred to patient studies. This strategy is also very efficient for MR sequence development as there is no need to be skilled on two very different environments and programming languages for the progression of the project. In many cases of translational research, 3 T small animal

Abbreviations: MR(I), Magnetic Resonance (Imaging); ECG, Electrocardiogram; FLASH, Fast Low Angle Shot; GRE, Gradient Echo; RV/LV, Right/Left Ventricle; TR/TE, Repetition time/Echo time; SNR, Signal to Noise ratio; rf, radio frequency; OCT, Optimal Cutting Temperature compound; NBT, Nitrobluetrazolium chloride; MMP-9, matrix metalloproteinase; sd, standard deviation; SI, signal intensity; ESV, end-systolic volume; EDV, end-diastolic volume; EV, ejection volume; EF, ejection fraction; ICC, Intraclass Correlation Coefficient; PSIR, Phase Sensitive Inversion Recovery; PC, Phase contrast.

* Corresponding author at: Department of Radiology, Department of Radiology and Medical Informatics,Geneva University Hospitals, 4 rue Gabrielle-Perret-Gentil, 1205 Geneva, Switzerland.
E-mail addresses: Lindsey.crowe@unige.ch (L.A. Crowe), Fabrizio.Montecucco@unige.it (F. Montecucco), federico.carbone@edu.unige.it (F. Carbone), iris.friedli@unige.ch (I. Friedli), Anne-Lise.HachullaLemaire@hcuge.ch (A.-L. Hachulla), Vincent.Braunersreuther@hcuge.ch (V. Braunersreuther), Francois.Mach@hcuge.ch (F. Mach), Jean-paul.vallee@hcuge.ch (J.-P. Vallée).

http://dx.doi.org/10.1016/j.mri.2017.07.024
0730-725X/

protocols can be easily adapted to the following patient study as already shown [1]. In the case of cardiac imaging, small animal studies on clinical MR systems have been successfully used by many groups [2]. Important results have been achieved, for example, in measurement of mass and function in cardiac hypertrophy [3], in quantification and characterization of myocardial infarct with manganese enhanced MRI [4,5], for iron oxides labeled monocytes [6] or gadolinium enhancement [7–10] in rat and mouse models with clinical MR systems.

Clinical 3 T scanners also have disadvantages such as lower SNR and weaker gradients. For cine, traditionally 2D, this implies limitation of spatial resolution (slice thickness) and temporal resolution (with a TR of over 10 ms [10]). Additionally, cardiovascular applications suffer from flow artifacts related to the relatively long echo times [7]. However, advances in clinical gradient hardware mean that the technical gap between low and high field systems is shrinking and careful choice of acquisition schemes and parameters can optimize low field systems for small animal imaging without the expense of additional equipment.

3D cine has the potential to overcome restrictions due to clinical MRI system hardware, compared to higher performance small animal systems. Isotropic resolution is available with 3D acquisitions, as opposed to the relatively large slice thickness necessary for 2D. In addition, since no slice selection gradient is needed for the 3D cine, the radio frequency excitation pulses can also be shortened to reduce repetition and echo times (TR and TE) to shorter than those achievable with 2D cine. The reduction in TR gives higher temporal resolution, particularly advantageous for the fast rodent cardiac cycle, and the decreased TE reduces flow artifacts in the cavities compared to those observed in 2D [7]. 3D cine has already been tested on high field systems, [11–13] but feasibility and performance on clinical 3 T MR systems are not known. In addition, one limitation of 3D cine is the low contrast between the blood and the myocardium. Previous investigators have used iron oxides and radial acquisition to enhance the contrast of 3D cine on small animal high field MR systems [14,15]. However, iron oxides, due to their size, require an intravenous access for injection, remain mainly intravascular and do not enhance significantly infarct area. This is contrary to gadolinium based contrast agents, which can be injected intraperitoneally with a rapid absorption in the vascular compartment and can delineate myocardial infarct as well as providing the necessary blood-myocardium contrast. Therefore, we were interested to test the effect of gadolinium based contrast media injection on 3D cine at 3 T to improve the contrast between the blood and the myocardium and to detect myocardial infarct.

The aim of this study was to validate a '4D strategy' on a 3 T clinical MR system using a 3D cine protocol after gadolinium injection and to compare functional assessment to 2D cine in mice. The performance for infarct size at 3 T was compared to histology and post-mortem imaging.

2. Methods

2.1. Mouse ischemia and reperfusion protocol

C57BL/6J mice, aged 8–12 weeks with a bodyweight range 24–28 g, were used in this study. The investigation conformed to the guidelines from Directive 2010/63/EU, from the National Institutes of Health (updated 2011) and has been approved by the local and Swiss authorities. Mice were submitted to a surgical protocol of cardiac ischemia and reperfusion as previously described [16,17]. Controls had no surgery. Groups consisted of 14 infarct mice plus 4 controls for function assessment, and 6 infarct mice plus 6 controls for histological comparison to MRI and reproducibility. For the infarct group, mechanical ventilation was performed (tidal volume 300 μl) using a rodent respirator (Minivent model 845, Hugo Sachs Elektronik, Harvard Apparatus, Germany). Anesthesia was maintained with 2% isoflurane in 100% O_2 through the ventilator. During surgery anesthesia was monitored by careful visual and tactile control of mouse consciousness (i.e. breathing rate and volume, heart rate, sweating and tearing). Mouse body temperature was monitored and maintained at 37 °C. A thoracotomy was performed and the pericardial sac was removed. An 8–0 prolene suture was passed under the left anterior descending (LAD) coronary artery at the inferior edge of the left atrium and tied with a slipknot to produce the occlusion. A small piece of polyethylene tubing was used to avoid damaging the artery during ligature. Ischemia was confirmed by the visualization of blanching myocardium, downstream of the ligation. After 60 min, the LAD coronary artery occlusion was released, allowing reperfusion. This was confirmed by visible restoration of color to the ischemic tissue. The chest was closed and air was evacuated from the chest cavity. The tracheal tube was then removed and normal respiration restored.

The mice were imaged by MR 24 h after the surgical procedure and were sacrificed via KCl injection to perform post mortem imaging (with the heart in diastole) and cardiac histological analyses of infarct size and immunohistology. Serum was collected to measure cardiac Troponin I levels.

2.2. MR imaging

Imaging was performed on a clinical 3 T MR scanner (Magnetom PRISMA, Siemens Medical Solutions, Erlangen Germany) with a dedicated 2-channel mouse heart receiver coil (Rapid Biomedical GmbH, Rimpar, Germany). Respiratory and ECG monitoring and triggering control was achieved by an external trigger set-up (S.A. Inc., Stony Brook, US).

After anesthesia induction (isoflurane), the Gadolinium contrast agent, Dotarem (0.01 mmol), was injected IP once the animal was in position. This dose is equivalent to 0.33 mmol/kg, on the same order as the clinical dose of 0.1–0.2 mmol Gd/kg in agreement with previous studies ([18,19]). The 3D cine was started a few minutes after injection and the 2D cines immediately afterwards. Anesthesia was maintained with 2% isoflurane during imaging. A cover was used to maintain a stable body temperature. Heart and respiratory rates were monitored and kept constant and with a similar range for all the animals via small adjustments of the isoflurane concentration (typical 35/min and HR 450 bpm). All animals were kept under stable and similar aesthesia levels. The acquisition window for the prospective ECG gating was set to 95% cardiac cycle to ensure coverage of the diastolic phase.

Protocol parameters are summarized in Table 1. The double ECG and respiratory triggered 3D FLASH gradient echo cine sequence proposed as a 4D strategy in this study had an acquired isotropic resolution of 344 μm. Due to the slab-selective rf in 3D and the use of an asymmetric echo, the TR and TE could be shortened to 7.8 and 2.9 ms respectively. Acquisition time was 25–35 min depending on respiration and heart rate. 15–22 cine phases were acquired depending on heart rate. The k-space order of the 3D scan was linear, with center of k space acquired at the midpoint of the acquisition.

For comparison, the previously optimized and validated conventional 2D FLASH cine sequence [5] had the same in-plane resolution of 344 μm, but a slice thickness of 1 mm. TR and TE were longer at 11 and 5.4 ms, respectively. This 2D cine had 10 consecutive short-axes covering right and left ventricles plus single 2- and 4-chamber views for an acquisition time of 20–25 min plus 5 min for pilot scans and slice positioning. 12–17 cine phases were acquired depending on heart rate.

After the in vivo MRI protocol, animals were sacrificed by injection of KCl. Post-mortem MRI was completed in 6 cases (5 infarct, 1 control). This consisted of a 3D FLASH GRE with a higher isotropic resolution of 130 μm and an acquisition time of 16 min. A 2-min low-resolution 3D scan was acquired before and after this long 3D to verify if any muscular contraction occurred during the longer scan.

2.3. Immuno- and nitrobluetrazolium chloride staining

Serum Troponin level was measured from blood samples taken the same day as MRI. For histological analysis, hearts of all 12 mice (control

Table 1
MRI sequence parameters.

	3D FLASH GRE cine	2D FLASH GRE cine	Post mortem 3D
Resolution (μm)	344 * 344 * 344	344 * 344 * 1000	130 * 130 * 130
FOV (mm)	66	66	66 * 55
Number of slices	60	4C, 2C, 10* SA	64
Bandwidth (Hz/pixel)	347	195	130
Flip angle (°)	30	30	30
TR (ms)	7.8	11.0	17.9
TE (ms)	2.9	5.4	9.8
Cine phases	15–22	12–17	n/a
Acquisition time (minutes)	25–35	20–25 + 5 pilot and slice positioning	16
	Asymmetric echo, slab selective rf, rf spoiling	Rf spoiling	Rf spoiling

and infarct) were removed immediately after MRI, frozen in cryo-embedding media 'Optimal Cutting Temperature compound' (OCT) and cut serially from the occlusion locus to the apex in 7 μm sections. Immunohistology for CD68+ (macrophages, primary Ab from ABD Serotec, Kidlington, UK) and matrix metalloproteinase (MMP)-9 (primary Ab from R&D Systems, Inc., Minneapolis, MN) was performed as previously described [20] on 9 ventricular cardiac sections per animal. Nitrobluetrazolium chloride staining (NBT) was performed to identify metabolically inactive tissues. Infarct size (I) was quantified as the NBT-negative area using MetaMorph software. Infarct volumes were reported as %I/V, i.e. percentages of stained area on total heart surface area for MMP-9 and percentage of unstained area on total area for NBT. The number of infiltrating cells per mm^2 of total heart surface area was quantified for macrophages (CD68+).

2.4. Image analysis

The 3D cine was reconstructed for analysis in the same orientation as the 2D cine images, but maintaining the acquired isotropic 344 μm resolution. The 2D cines were analyzed as acquired.

Flow artifact was assessed by both visual scoring and quantification of residual artifactual signal in the center of the left ventricle at the level of the papillary muscles. Visual scoring of artifacts was divided into classification as moderate (drawing of endocardial volumes more challenging) or severe (volume analysis not be possible for that phase). The percentage of the cardiac cycle affected by artifacts was calculated (phases with artifact / total number of phases). For the objective quantitative evaluation of the flow artifact, we defined the 'sd/SI ratio' (expressed as a percentage), the standard deviation of blood signal in each phase, i, compared to the mean artifact free signal in the first cardiac phase, 0, that is sd(i)/SI(0). This value was calculated as a mean for 2D and 3D, and compared via ANOVA for the mean per animal.

Cardiac function was analyzed using Osirix software (Open source http://www.osirix-viewer.com/). End-systolic (ESV), end-diastolic (EDV) volumes, ejection volume (EV) and fraction (EF) were calculated by manually tracing end-systolic and end-diastolic endocardial contours on all short axis images covering left and right ventricle (LV and RV). The papillary muscles were not included in the regions. 2D and 3D volumes were first compared separately for right and left ventricles, for systole and diastole and then pooled altogether for a correlation between 2D and 3D values. Left ventricle epicardial contours were also used to calculate myocardial mass of the LV including the septum. These mass values were measured in diastole.

MR infarct volume was similarly manually segmented. As with histology, the infarct volume as a percentage of total tissue volume was calculated (%I/V). These were compared to NBT and the other histological markers described in Section 2.3.

For all statistical analysis, SPPS (version 21) was used. R^2 and p values were given for linear correlations. ANOVA was used to compare flow artifacts in 2D and 3D and paired *t*-tests were also used to compare volumes. Significant difference was defined as $p < 0.05$. 3D volumes were repeated for both inter- and intra-observer reproducibility with correlation and ICC. Regions were redrawn in a blinded fashion by the same observer and a second observer after an interval of several months.

3. Results

3.1. Image quality and acquisition time

The in vivo protocol acquisition was successful in all the animals. The blood to myocardium contrast-to-noise ratio (CNR) was high, allowing easy endocardial delineation in both 2D and 3D (CNR 80 and 30 respectively). Image quality was good for both 2D and 3D with better apical and right ventricular volume (RV) delineation from isotropic whole heart coverage in 3D (Fig. 1). The shorter TR in 3D gave better definition of the cardiac phases with increased temporal resolution (on average, 18 c.f. 13 cardiac phases). The mean heart rate was not different between the control and infarct groups and was maintained as stable as possible with control of the anesthesia at around 450 beats per minute.

To cover the whole heart with isotropic resolution in 2D (three times the number of acquisitions) would be prohibitive in terms of overall scan time without considering the necessity for signal averaging for SNR. For 2D imaging, scan times were 20–25 min for cine plus planning and would be 35–45 min for cine plus Gadolinium enhanced 2D PSIR needed for infarct quantification. 3D cine required no complex planning of image planes and allowed retrospective display and analysis of any chosen plane or slice group. For 3D imaging, the total scan time was 25–35 min, depending on the heart rate and respiratory rate, for the full volume cine and infarct quantification in a single acquisition.

Supplemental Digital Content 1a and b consist of 3D and 2D cine images for a normal (a) and an infarct (b) mouse for dynamic visualization of the images.

3.2. Flow artifact

Flow artifacts were present in both the 2D and 3D cine images. Fig. 2 shows comparison of four chamber and short axis images from 2D and 3D acquisitions. Only one third of the cine phases are shown for clarity, but making sure to illustrate the most severe artifacts. In general, the most severe artifacts were in the late phases of the cardiac cycle after systole, i.e. those that were not used for the volume and mass calculations. Flow artifact was visually reduced in 3D cine compared to 2D cine and also appeared to be more central in the LV cavity not reaching the endocardial borders.

By visual scoring, the artifacts on the 2D cines were severe in 31% of cardiac phases and moderate in 14%. For the 3D cine, the percentage of phases with severe artifact was only 2%, with 20% having moderate artifact. This showed a significant advantage of the 3D cine over the 2D cine ($p < 0.0001$). Further objective quantification using the sd/SI ratio gave similar results to the qualitative assessment. The mean sd/SI ratio per animal was significantly higher in 2D cine (17% ± 5%) than in 3D cine (13% ± 3%) ($p = 0.008$) indicating less severe artifacts in the 3D images.

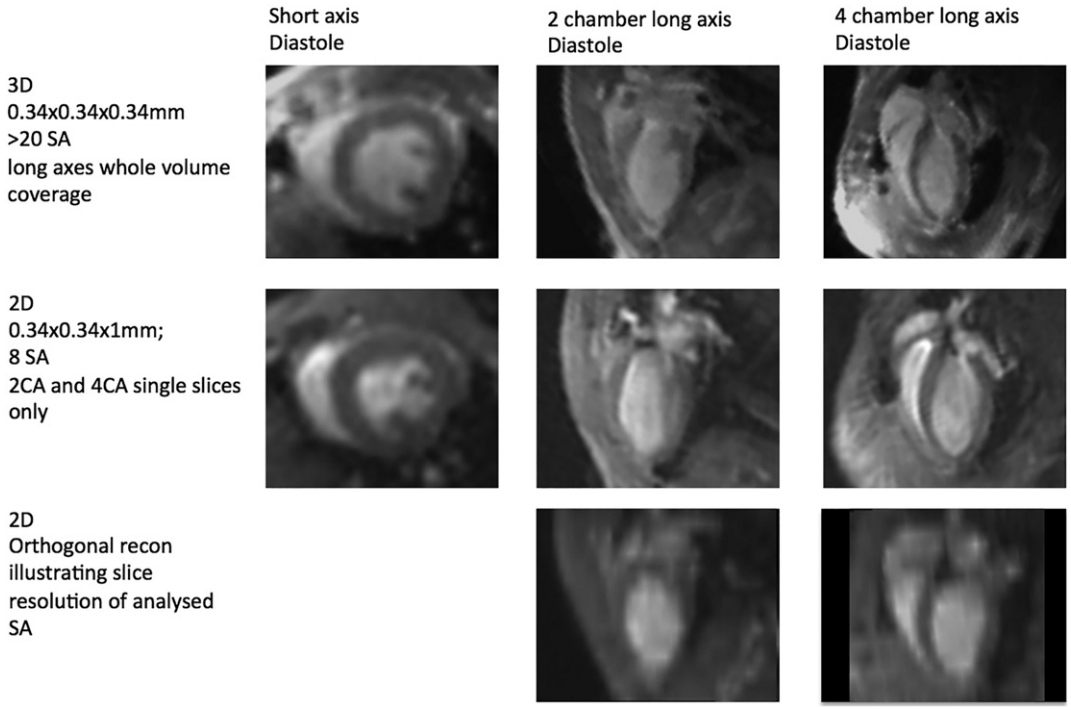

Fig. 1. *Image Quality*. Images showing the comparison of image quality in a normal heart (slice resolution and contrast) in 2D and 3D sequences. Cine phases from a 3D GRE acquisition with isotropic resolution of 344 μm and TR/TE 7.8/2.9 ms and from a 2D GRE acquisition with 344 μm in plane resolution and 1 mm slice thickness, TR/TE 11/5.4 ms. The reconstruction of the classic imaging planes from the 3D acquisition, the acquired 2D images and the corresponding reconstruction to show the slice thickness and coverage of the 2D short axis stack are illustrated. Image quality and contrast as acquired shows excellent comparison; lack of apex definition is visible on the orthogonal reconstruction that would not be evident in the original acquired short axis stack.

3.3. LV and RV volumes and function

All the volume and function results are summarized in Table 2. By comparison to 3D cine, 2D cine underestimated LEDV, LESV, REDV, RESV. This resulted in a slightly higher ejection fraction in the 2D cine for both ventricles (except RV in the infarct group). However, there was a strong correlation between 2D and 3D for all volumes as well as the EF and EV ($R^2 > 0.46$ $p \leq 0.001$).

A further internal validation was obtained by the comparison of the left and right ejection volumes, which should be equal in this mouse

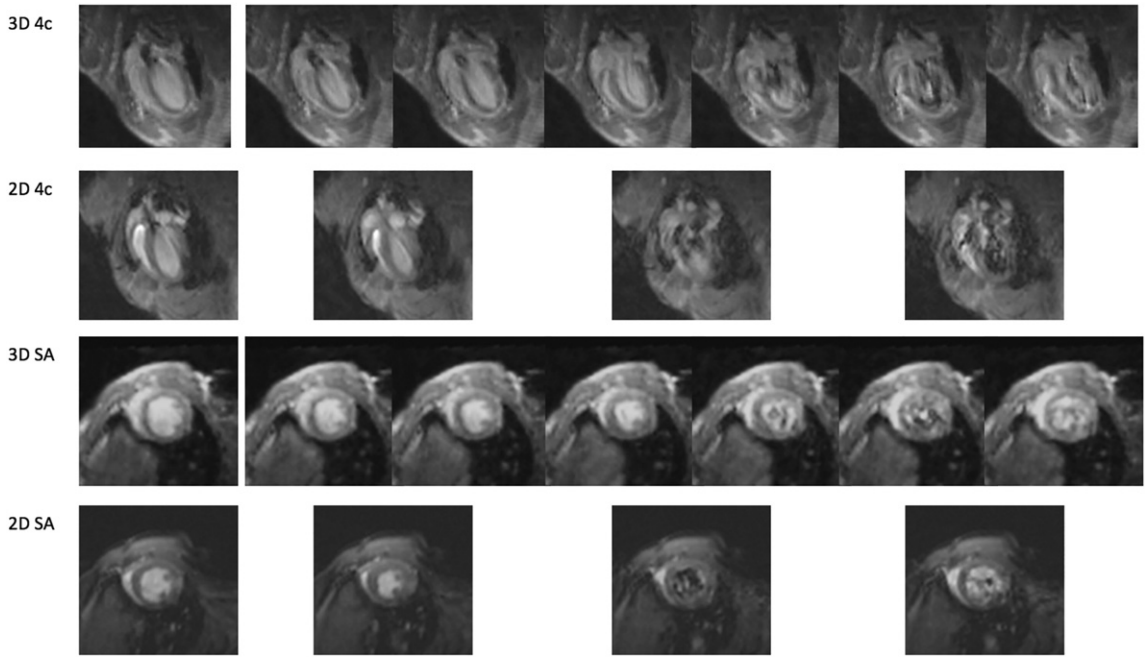

Fig. 2. *Flow artifacts*. Four-chamber and short axis images showing the comparison of flow artifacts in 3D and 2D sequences in a normal mouse heart. Around one third of the cine phases (including the most severe artifacts) are shown for clarity. 3D GRE acquisition with isotropic resolution of 344 μm and TR/TE 7.8/2.9 ms. 2D with 344 μm in plane resolution and 1 mm slice thickness, TR/TE 11/5.4 ms.

Table 2
2D vs 3D left and right ventricular volumes; EDV (end diastolic volume) and ESV (end systolic volume), ejection volumes (EV) and ejection fractions (EF) with correlations and paired *t*-tests for normal, infarct and all mice together (significance defined as $p < 0.05$).

2D versus 3D		Controls		Infarct		All mice					
		Mean ± sd mm^3	p of paired *t*-test	Mean ± sd mm^3	p of paired *t*-test	Mean ± sd mm^3	p of paired *t*-test	Regression slope	Intercept	R^2	p of correlation
Left EDV	3D	76.28 ± 17.79	0.541	62.15 ± 13.20	0.247	65.29 ± 15.02	0.21	0.54	26.49	0.48	0.001
	2D	69.45 ± 5.48		59.80 ± 12.31		61.94 ± 11.76					
Left ESV	3D	38.10 ± 12.39	0.493	36.59 ± 11.91	0.46	36.93 ± 11.66	0.278	1.04	−4.19	0.58	<0.0005
	2D	32.63 ± 3.45		34.69 ± 18.03		34.23 ± 15.86					
Left ejection volume	3D	38.18 ± 7.29	0.792	25.56 ± 8.71	0.859	28.36 ± 9.82	0.764	0.92	1.66	0.50	0.001
	2D	36.83 ± 6.22		25.11 ± 13.06		27.71 ± 12.74					
Left ejection fraction	3D	51.03 ± 8.19	0.757	41.55 ± 13.39	0.612	43.66 ± 12.86	0.542	1.35	−13.38	0.67	<0.0005
	2D	52.83 ± 6.12		43.49 ± 23.65		45.56 ± 21.22					
Right EDV	3D	60.18 ± 13.04	0.151	48.81 ± 11.39	0.005	51.34 ± 12.36	0.001	0.56	13.88	0.47	0.002
	2D	50.80 ± 10.65		40.33 ± 8.99		42.66 ± 10.09					
Right ESV	3D	24.48 ± 15.09	0.184	24.47 ± 7.22	0.204	24.47 ± 8.95	0.055	0.65	4.47	0.34	0.011
	2D	15.78 ± 7.67		21.59 ± 10.29		20.30 ± 9.87					
Right ejection volume	3D	35.70 ± 4.37	0.854	24.34 ± 8.42	0.021	26.86 ± 9.01	0.025	0.86	−0.80	0.50	0.001
	2D	35.05 ± 6.14		18.74 ± 9.16		22.37 ± 10.93					
Right ejection fraction	3D	61.53 ± 15.30	0.228	49.42 ± 12.27	0.557	52.11 ± 13.54	0.996	1.02	−1.09	0.46	0.002
	2D	70.20 ± 10.91		46.96 ± 19.64		52.12 ± 20.37					

model. Paired *t*-test comparing EV left to right showed no significant difference for 3D ($p = 0.37$), nor 2D ($p = 0.30$) grouping all animals. For correlations, the slopes of left to right EV for both 2D and 3D were 1.17 ($R^2 = 0.75$) and 1.05 ($R^2 = 0.50$) showing good correlation and equality. The slope tended to be closer to 1 for 3D, but the slopes were not significantly different from each other, and neither 2D or 3D significantly different from a slope of 1.

None of the functional parameters, except LV ESV and LV EF, were different between the infarct and normal groups. This may result from the fact that the model was only at 24 h post reperfusion and the majority of the infarcts were small. Values obtained were in reasonable agreement with literature [5]. In the ischemia/reperfusion group, anterolateral hypokinesia or akinesia was consistently observed in both 2D and 3D cines (Fig. 3), but visually better delineated on 3D cines due to increased temporal and spatial resolution.

3.4. Reproducibility

Intra observer reproducibility was generally higher than inter observer reproducibility (significant increase in ICC, $p < 0.01$) and 3D performed better than 2D for inter observer (significant increase in ICC, $p < 0.01$) with equal high performance for 2D and 3D intra observer (no statistical difference). Intraclass correlation coefficients with p values are given in the Table 3.

3.5. Mass and postmortem images

Post mortem scans (GRE with an isotropic resolution of 130 μm) were successful in 6 mice (5 infarct and one normal) and are shown as part of Fig. 4. A fast 3D scan repeated before and after the high resolution 3D scan post mortem was different in a further 6 cases showing

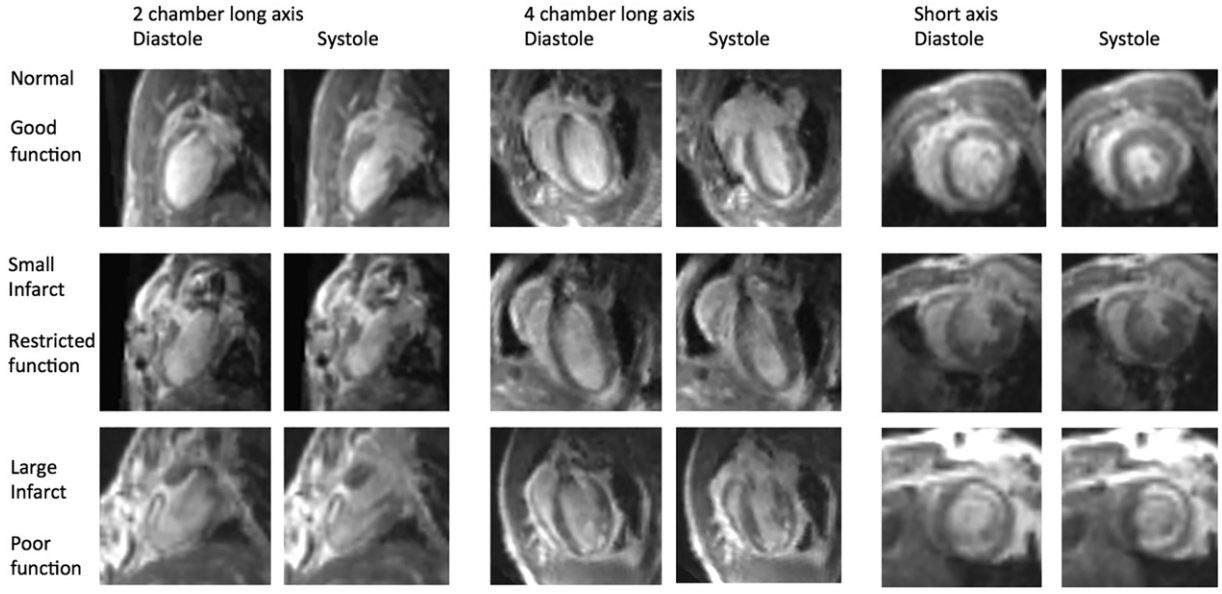

Fig. 3. *Functional assessment: Effect of Infarct.* 3D cine phases from a GRE acquisition with isotropic resolution of 344 μm and TR/TE 7.8/2.9 ms. Function differences (comparing systole and diastole in each imaging plane) between a normal and an infarct with visualization of the enhanced infarct region on the 2-chamber view. Examples show no infarct and good function, small infarct and restricted function and large infarct with poor function.

Table 3
Intraclass correlations (ICC) and p values (significant $p < 0.05$) for inter and intraobserver reproducibility for measured volumes and calculated functional parameters.

	Intra 3D		Inter 3D		Intra 2D		Inter 2D	
	ICC	p	ICC	p	ICC	p	ICC	p
Left diastolic volume	0.99	<0.0005	0.99	<0.0005	0.99	<0.0005	0.94	<0.0005
Left systolic volume	0.94	<0.0005	0.95	<0.0005	0.97	<0.0005	0.86	<0.0005
Left ejection volume	0.83	<0.0005	0.71	0.003	0.94	<0.0005	0.25	0.20
Left ejection fraction	0.76	0.001	0.63	0.01	0.92	<0.0005	0.35	0.12
Right diastolic volume	0.90	<0.0005	0.82	<0.0005	0.96	<0.0005	0.33	0.14
Right systolic volume	0.92	<0.0005	0.84	<0.0005	0.98	<0.0005	0.62	0.01
Right ejection volume	0.88	<0.0005	0.60	0.01	0.82	<0.0005	0.20	0.26
Right ejection fraction	0.92	<0.0005	0.74	0.002	0.84	<0.0005	0.40	0.09

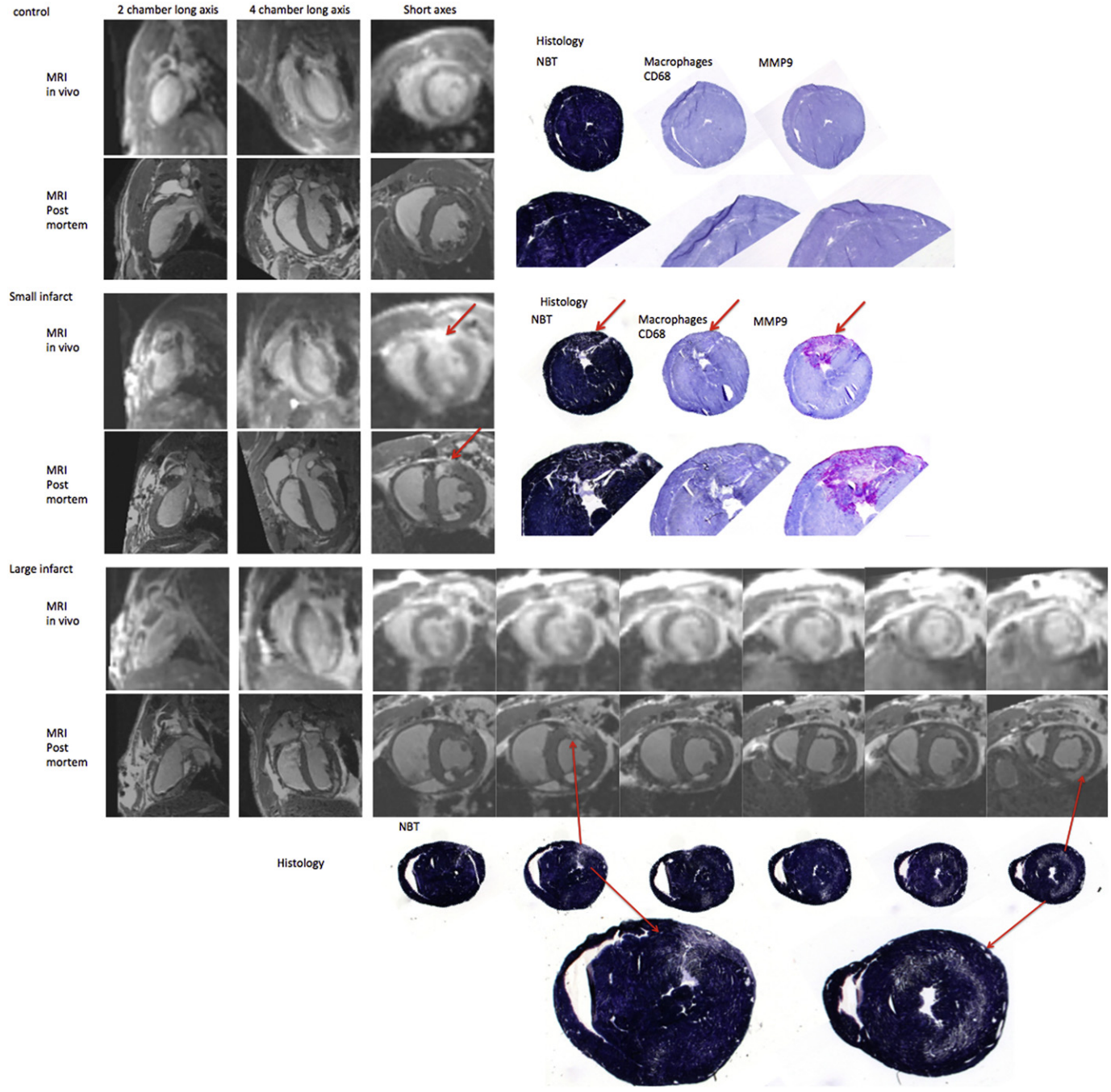

Fig. 4. *Infarct visualization*. 3D in vivo and post mortem images showing zero, small and large infarcts. 4 chamber, 2 chamber, mid and apical short axes for three mice along with corresponding histological pictures of macrophages (CD68+), MMP-9 and NBT showing excellent agreement between MRI and the gold-standard infarct staining.

Table 4
Mean and standard deviation values for myocardial mass (left ventricle mass including septum).

	Control (only 1)	Infarct	All mice
	Mass mean mm^3	Mass mean ± sd mm^3	Mass mean ± sd mm^3
Post mortem	87.1	83.5 ± 3.1	84.1 ± 3.2
2D in vivo diastole	95.5	84.8 ± 7.2	86.6 ± 7.8
3D in vivo diastole	90.7	87.1 ± 8.8	87.7 ± 8.0
2D in vivo systole	91.3	82.5 ± 6.3	83.9 ± 6.7
3D in vivo systole	88.0	82.2 ± 9.9	83.2 ± 9.2
	Correlation slope	Correlation R^2 (p)	*t*-Test p
2D vs 3D in vivo	0.83	0.73 (0.03)	0.53
Post mortem vs 3D in vivo	1.00	0.44 (0.03)	0.24

that the heart had contracted during the long 3D high-resolution acquisition and the post mortem scan was deemed to be unreliable for morphology quantification. Mass values are given in Table 4.

Correlation between 2D and 3D LV mass in vivo was good (slope 0.83, $R^2 = 0.73$, $p = 0.03$ with no statistical difference $p = 0.53$). The postmortem static high-resolution MR images were used as a 'gold standard' for comparison to 3D in vivo, due to their higher spatial resolution and lack of motion blurring. There was no significant difference between post mortem and 3D in vivo LV mass with $p = 0.24$, with an excellent correlation of slope 1 ($R^2 = 0.44$ $p = 0.03$).

3.6. Infarct correlation

In vivo and post mortem 3D images of three mice are shown in Fig. 4 (4-chamber, 2-chamber and mid and apical short axes). The first mouse shown had no infarct, the second a small transmural infarct, and the third a large apical infarct (with sub-endocardial sparing) as well as a small transmural infarct near the site of the occlusion. These fine details of the infarct morphology were clearly visible in vivo and were confirmed by the higher resolution post mortem scans and histology. For quantitative comparison, the mean infarct volume was expressed as a percentage (%I/V) to account for scaled absolute volume difference for both the total myocardium and the infarct on fixing. Overall, 2 mice had a larger infarct covering 6–12% of the full apex and the other 5 had smaller infarcts localized in the basal region of 2–5% leading to a %I/V for MRI in vivo over all infarct mice of 5% ± 3%. In vivo MRI (%I/V) was very accurate to measure infarct volume with a strong correlation (Fig. 5) to both %I/V NBT ($y = 1.00x + 0.18$, $R^2 = 0.90$, $p < 0.0005$) and %I/V post-mortem MRI ($y = 1.10x + 0.17$, $R^2 = 0.997$, $p < 0.0005$). There was also an excellent correlation for infarct volume (%I/V) between postmortem MRI and NBT at $y = 0.98x + 0.84$, $R^2 = 0.89$, $p = 0.005$. For paired *t*-test, the p value showed no significant difference with $p > 0.2$ for all three comparisons. Fisher z-test also shows that the regression slopes are not significantly different to 1 (i.e. $y = x$).

The absolute infarct volumes from both MRI and NBT also correlated with systemic troponin levels with $R^2 = 0.93$, for MRI and $R^2 = 0.80$ for histology NBT. Similarly, quantification of macrophages (CD68+ cells/mm^2) correlated with MRI %I/V $R^2 = 0.62$ and histology %I/V $R^2 = 0.69$ ($p < 0.0005$). MMP-9 (%) correlated with $R^2 = 0.86$ ($p < 0.0005$) to MRI %I/V and $R^2 = 0.78$ ($p < 0.0005$) to histology %I/V. Images are shown in Fig. 4. In addition, left ejection fraction showed a negative correlation with MRI infarct volume (%I/V) with $R^2 > 0.3$. The Supplemental Digital Content 2 video shows cine images including a large apical, non-transmural infarct and a small infarct near the ligated coronary in the 3 conventional planes.

4. Discussion

In summary, this study introduces a '4D strategy' of a 3D isotropic volume with temporal cine imaging for function and infarct size assessment in rodent on a clinical 3 T scanner. Unlike conventional 2D cine, there was no need for complex, time-consuming slice planning. This technique compared well to 2D cine for functional assessment with the advantage of better coverage of both ventricles. Ejection volume measurement was accurate for left and right ventricles allowing internal validation using the physiological right to left equality in mice. Secondly, gadolinium contrast injection allowed infarct to be quantified and agreed very well with histological analysis. The gadolinium was injected for the blood/myocardium contrast and not specifically for infarct detection as 3D dynamic (4D) functional cardiac imaging in clinical studies often recommends the use of gadolinium for improved blood SNR [21].

4.1. Reduced flow artifact

The shorter TE allowed by the 3D RF excitation pulse (duration 0.5 ms for 3D compared to 2 ms for 2D) and asymmetric echo leads to reduced flow artifacts, and better analysis of the myocardial wall over the whole cardiac cycle (3D TE 2.9 compared to 5.4 ms for 2D). The use of half echo time with our sequence could provide a potential benefit with addition TE reduction. Kramer et al. recently used this technique in a 2D cine on a 3 T clinical MR system with a center-out radial readout [22]. This 2D study used a self-navigating technique with

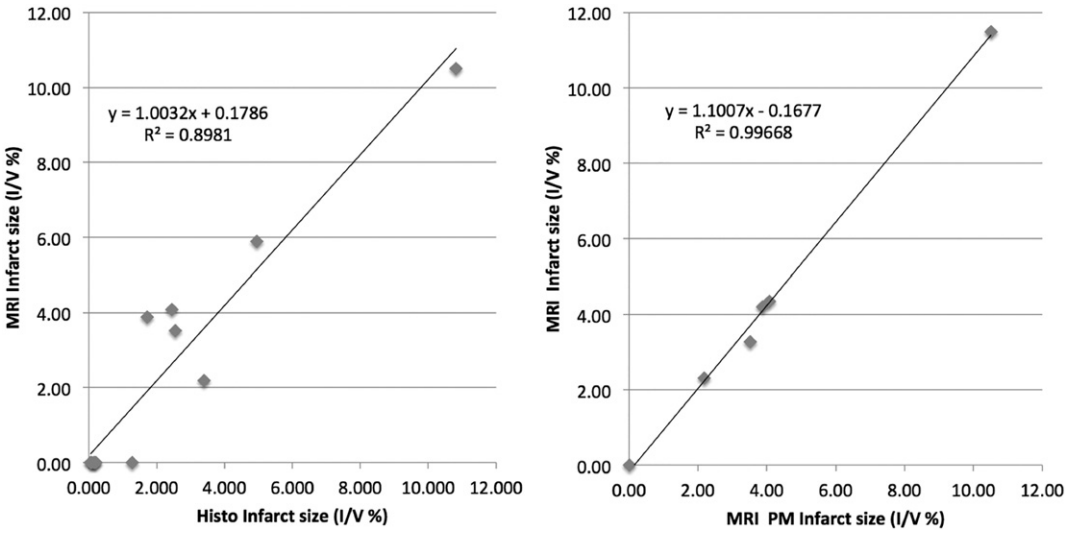

Fig. 5. *Infarct quantification.* MRI/Histological correlations for (a) percentage infarct size on 3D cine (diastole) and NBT quantification, and (b) correlation in vivo vs post mortem for MRI.

excellent cine quality, however with some flow artifacts remaining [22]. Flow artifact could also potential be reduced using a black-blood cine [23]. This is however more complex for a 3D volume [24,25] where thick slabs may result in poor blood signal nulling [12].

4.2. Improved temporal resolution

The shorter 3D excitation pulse and asymmetric echo also allowed improved temporal resolution by around 50%. The 3D value was similar to that obtained from other methods such as interleaved cine and temporal regularization with TR 6.8 ms [26] and the half echo with TR 6.5 ms [22]. Better functional definition of the short systolic period and decreased blurring of the fine structure particularly of the RV wall are obtained. Several techniques, including the radial self-gated method reported at 3 T [22] and interleaved cine acquisitions [26], involve the use of a 'sliding window' for increasing temporal coverage of the cardiac phases. These methods lead to some averaging of lines from different phases of the cardiac cycle to produce the frames of the cine series. Cine frames therefore have higher effective temporal resolution, but are not truly independent in time and may be susceptible to cardiac motion blurring. In the 3D cine acquisition, the shorter TR and TE were a consequence of the shortened rf pulse and all k-space lines were acquired for each phase ensuring the absence of cardiac motion and no data sharing between cine frames.

4.3. Improved spatial resolution for ventricular assessment

In general 3D measured volumes were larger than those derived from 2D cines. This can be explained by the fact that basal slices are better visualized on the 3D images. Partial volume effects of the thicker slices in 2D meant that the definition of smaller structure at the base of the RV was lost and the segmentation did not include the final slices visible in 3D. With the thinner slices in 3D it was also easier to accurately include the right ventricular outflow tract that, depending on the slice position can be partially or completely included in 2D segmentation leading to variability. Flow artifacts can also obscure the valve level in the 2D cine and there is the possibility of misregistration between short axes acquired in separate scans. All this results in more accurate values for 3D RV volume, but can also lead to a difference for the functional parameters between 2D to 3D.

Improved spatial resolution is a significant advantage of 3D cine allowing better RV assessment as well as internal validation of EV equality left to right for accurate volume measurements.

The ejection fraction values in this study can be considered slightly low for the control group compared to the literature [3]. It is important to note that that the 3D and 2D techniques both showed the low EF. The EF is therefore self-consistent and also in agreement with previous studies using the same 2D protocol in our laboratory [5,20,26] inferring it is not an error with the 3D method. The most likely explanation of these low values could be an effect of anesthesia. The isoflurane levels (2%) were higher than some of the reported studies with high injection fraction (1%) [3] and the ECG set up and scan time significantly longer than the 15–30 min, which could explain the reduction in EF [3], which could cause >20% reduction in EF [27].

4.4. Infarct assessment

Late gadolinium enhancement is a well-established technique to quantify infarct size [8–10]. In this study, intraperitoneal Gd was used for blood to tissue contrast, but also provided uptake in the infarct region on the 3D cine images. Therefore, despite the absence of an PSIR acquisition in this study we have accurate infarct volumes comparable to literature [28,29] and validated to histological quantification in this study. The combined late enhancement and cine also shows potential for the assessment of salvageable myocardium, where there is a contraction and perfusion deficit but no gadolinium uptake [30]. An interesting point is the absence of visualization of contrast accumulation in the infarct by the 2D cine. The 2D was always carried out after the 3D and therefore under different conditions in terms of time post gadolinium. However, in the post mortem cases, the LGE was still visible after the 3D and 2D in vivo imaging. Successful late gadolinium enhancement has been reported as acquired 30 min after injection [18], which is consistent with the timing of the 2D imaging in our case. The shorter TE and TR in the 3D will also emphasize the T1 contrast in comparison to the 2D cine.

In 2 out of 6 mice, non-transmural infarcts were observed with significant subendocardial sparing, with this thin band emphasizing the high resolution. This in vivo MRI pattern, confirmed by histology, is very different from the usual clinical pattern of infarct but has been already reported in mice [31–33]. It may be related to direct oxygenation of the sub endocardium from the blood of the LV.

4.5. Scan time

For 2D imaging, scan times were 20–25 min for cine plus planning and would be 35–45 min for cine plus the multislice Gadolinium enhanced 2D PSIR needed for infarct quantification. Therefore for a full assessment of function and infarct enhancement the 3D technique at 25–35 min more than compensates the time penalty of 3D compared to 2D cine as it provides all the necessary data in one acquisition with minimal time for slice planning. The 3D cine at clinical field is highly competitive, with scan times and resolution on the same order of those reported in the literature, even studies at high field. A 3D cine study with iron oxide contrast injection in mice at high field [14,15] used protocols with a TE/TR of 0.05/3.5 ms and scan times of 12–26 min (156 μm isotropic resolution, 10 averages). Other 3D cine studies at 7 T compared bright and dark blood protocols (200 μm spatial resolution and 12 ms temporal resolution and a scan time of 20 min [12]) and variations of temporal and spatial resolution in a 30 min scan time (87 μm–352 μm slice thickness, and TR 4.8 ms–12.4 ms) [11]. In all these cases, the scan times given were similar to our own but included only functional data and not infarct enhancement. Feintuch [12] and Bishop [34] reported the possibility of 3D cine for multiple mouse imaging can make use of averaging in 3D retrospective gated cines using the advantages of the signal averaging properties.

4.6. Validation

The larger discrepancy in the 2D inter observer variability compared to 3D, although still good, can be explained by the ability to include or exclude a final basal slice confounded by possible flow artifacts and partial volume effect from the 2D slice thickness. A direct comparison study however, would not be affected by this systematic interobserver error, as the high intra observer reproducibility would ensure the same technique is used for all subjects.

A major limitation common to all new cine development studies is validation. Gold standard methods, such as weighing of dissected hearts is technically difficult, especially to remove attached fat and to split the left and right ventricles for correlation. Neither does this give information about function. Previous studies have used normal and hypertrophic mice, where volumes vary by a factor of 2 [26] to give a wider range of mass values for correlation. Often several 3D protocols have been compared between themselves or with validation to literature functional values [11,12]. A major advantage of our study is the original validation methods for the 3D cine using internal comparison of left and right ejection volumes and correlation with 2D cine, post mortem MRI and histology for infarct validation. Left to right correlation for 3D ejection volumes was verified, and confirmed accuracy of our 3D method.

4.7. Limitations of the study

This study contains a limited range of values as most mice had similar mass and function, with the difference being the absence or

presence of a small infarct and no remodeling of mass at 24 h post reperfusion. This time point was chosen due to its importance in treatment studies [35]. Statistical analysis using paired *t*-tests was therefore used. For the MRI and histological infarct comparison there is a wider range of values and a strong correlation. 3D reproducibility was excellent and the poorer 2D reproducibility may be improved with training to ensure accuracy in the extreme apical and basal slices.

One limitation of the acquisition of the cine after contrast injection is the poorer delineation of the sub-endocardial border in the infarcted area as known from clinical MRI. Although there is good normal to infarct myocardial contrast, the infarct can have similar intensity to the blood pool. However the sub-endocardial sparing in these mice that helped to differentiate blood and infarct myocardial signal. In addition, the cine acquisition also gave a dynamic information that aids the myocardium to blood delineation.

5. Conclusion

In conclusion, we validated a new 4D strategy based on 3D FLASH/GRE cine after contrast media injection in mice, where function and infarct information were obtained in a single scan after minimal slice planning. Isotropic 3D cardiac cine of mice on a clinical 3 T system improved coverage, and spatial and temporal resolution. Cardiac function was obtained for both LV and RV, the latter usually not quantifiable by 2D standard cine. Infarct quantification showed excellent correlation to histology. This sequence has the potential to replace 2D function and infarct techniques in rodents on clinical MR systems.

Supplementary data to this article can be found online at http://dx.doi.org/10.1016/j.mri.2017.07.024.

Funding

This work was supported in part by the Centre for Biomedical Imaging (CIBM) of EPFL, University of Geneva and the University Hospitals of Geneva and Lausanne, funded by the Swiss National Science Foundation via its financial support for the PRISMA MRI (R'Equip grants: SNF No 326030_150816)

This study was supported by European Commission (FP7-INNOVATION I HEALTH-F2-2013-602114; Athero-B-Cell: Targeting and exploiting B cell function for treatment in cardiovascular disease) to Prof. F. Mach. This work was supported by a Swiss National Science Foundation Grant to Prof. F. Montecucco (#310030_152639/1).

Acknowledgements

The authors wish to thank Dr. Bénédicte Delattre for helpful discussions, and Aline Roth and Fabienne Burger for technical assistance.

References

[1] Friedli I, Crowe LA, Berchtold L, Moll S, Hadaya K, de Perrot T, et al. New magnetic resonance imaging index for renal fibrosis assessment: a comparison between diffusion-weighted imaging and T1 mapping with histological validation. Sci Rep 2016;6:30088.
[2] Gilson WD, Kraitchman DL. Cardiac magnetic resonance imaging in small rodents using clinical 1.5 T and 3.0 T scanners. Methods 2007;43:35–45.
[3] Yang Z, Berr SS, Gilson WD, Toufektsian MC, French BA. Simultaneous evaluation of infarct size and cardiac function in intact mice by contrast-enhanced cardiac magnetic resonance imaging reveals contractile dysfunction in noninfarcted regions early after myocardial infarction. Circulation 2004;109:1161–7.
[4] Delattre BM, Braunersreuther V, Gardier S, Hyacinthe JN, Crowe LA, Mach F, et al. Manganese kinetics demonstrated double contrast in acute but not in chronic infarction in a mouse model of myocardial occlusion reperfusion. NMR Biomed 2012;25:489–97.
[5] Delattre BM, Braunersreuther V, Hyacinthe JN, Crowe LA, Mach F, Vallee JP. Myocardial infarction quantification with Manganese-Enhanced MRI (MEMRI) in mice using a 3 T clinical scanner. NMR Biomed 2010;23:503–13.
[6] Montet-Abou K, Daire JL, Hyacinthe JN, Jorge-Costa M, Grosdemange K, Mach F, et al. In vivo labelling of resting monocytes in the reticuloendothelial system with fluorescent iron oxide nanoparticles prior to injury reveals that they are mobilized to infarcted myocardium. Eur Heart J 2010;31:1410–20.
[7] Saleh MG, Sharp SK, Alhamud A, Spottiswoode BS, van der Kouwe AJ, Davies NH, et al. Long-term left ventricular remodelling in rat model of nonreperfused myocardial infarction: sequential MR imaging using a 3 T clinical scanner. J Biomed Biotechnol 2012;2012:504037.
[8] Coolen BF, Paulis LE, Geelen T, Nicolay K, Strijkers GJ. Contrast-enhanced MRI of murine myocardial infarction - part II. NMR Biomed 2012;25:969–84.
[9] Geelen T, Paulis LE, Coolen BF, Nicolay K, Strijkers GJ. Contrast-enhanced MRI of murine myocardial infarction - part I. NMR Biomed 2012;25:953–68.
[10] Voelkl JG, Haubner BJ, Kremser C, Mayr A, Klug G, Loizides A, et al. Cardiac imaging using clinical 1.5 T MRI scanners in a murine ischemia/reperfusion model. J Biomed Biotechnol 2011;2011:185683.
[11] Bucholz E, Ghaghada K, Qi Y, Mukundan S, Johnson GA. Four-dimensional MR microscopy of the mouse heart using radial acquisition and liposomal gadolinium contrast agent. Magn Reson Med 2008;60:111–8.
[12] Feintuch A, Zhu Y, Bishop J, Davidson L, Dazai J, Bruneau BG, et al. 4D cardiac MRI in the mouse. NMR Biomed 2007;20:360–5.
[13] Zhong X, Gibberman LB, Spottiswoode BS, Gilliam AD, Meyer CH, French BA, et al. Comprehensive cardiovascular magnetic resonance of myocardial mechanics in mice using three-dimensional cine DENSE. J Cardiovasc Magn Reson 2011;13:83.
[14] Trotier AJ, Castets CR, Lefrancois W, Ribot EJ, Franconi JM, Thiaudiere E, et al. USPIO-enhanced 3D-cine self-gated cardiac MRI based on a stack-of-stars golden angle short echo time sequence: application on mice with acute myocardial infarction. J Magn Reson Imaging 2016;44:355–65.
[15] Trotier AJ, Lefrancois W, Van Renterghem K, Franconi JM, Thiaudiere E, Miraux S. Positive contrast high-resolution 3D-cine imaging of the cardiovascular system in small animals using a UTE sequence and iron nanoparticles at 4.7, 7 and 9.4 T. J Cardiovasc Magn Reson 2015;17:53.
[16] Montecucco F, Bauer I, Braunersreuther V, Bruzzone S, Akhmedov A, Luscher TF, et al. Inhibition of nicotinamide phosphoribosyltransferase reduces neutrophil-mediated injury in myocardial infarction. Antioxid Redox Signal 2013;18:630–41.
[17] Akhmedov A, Montecucco F, Braunersreuther V, Camici GG, Jakob P, Reiner MF, et al. Genetic deletion of the adaptor protein p66Shc increases susceptibility to short-term ischaemic myocardial injury via intracellular salvage pathways. Eur Heart J 2015;36:516–26.
[18] Park C, Park EH, Chang K, Hong KS. Sector-based assessment of infarct size on late-gadolinium-enhancement MRI in a mouse model of acute myocardial infarction. Int Heart J 2016;57:736–41.
[19] Moreno H, Hua F, Brown T, Small S. Longitudinal mapping of mouse cerebral blood volume with MRI. NMR Biomed 2006;19:535–43.
[20] Braunersreuther V, Montecucco F, Pelli G, Galan K, Proudfoot AE, Belin A, et al. Treatment with the CC chemokine-binding protein Evasin-4 improves post-infarction myocardial injury and survival in mice. Thromb Haemost 2013;110:807–25.
[21] Dyverfeldt P, Bissell M, Barker AJ, Bolger AF, Carlhall CJ, Ebbers T, et al. 4D flow cardiovascular magnetic resonance consensus statement. J Cardiovasc Magn Reson 2015;17:72.
[22] Kramer M, Herrmann KH, Biermann J, Freiburger S, Schwarzer M, Reichenbach JR. Self-gated cardiac cine MRI of the rat on a clinical 3 T MRI system. NMR Biomed 2015;28:162–7.
[23] Berr SS, Roy RJ, French BA, Yang Z, Gilson W, Kramer CM, et al. Black blood gradient echo cine magnetic resonance imaging of the mouse heart. Magn Reson Med 2005;53:1074–9.
[24] Crowe LA, Gatehouse P, Yang GZ, Mohiaddin RH, Varghese A, Charrier C, et al. Volume-selective 3D turbo spin echo imaging for vascular wall imaging and distensibility measurement. J Magn Reson Imaging 2003;17:572–80.
[25] Crowe LA, Varghese A, Mohiaddin RH, Yang GZ, Firmin DN. Elimination of residual blood flow-related signal in 3D volume-selective TSE arterial wall imaging using velocity-sensitive phase reconstruction. J Magn Reson Imaging 2006;23:416–21.
[26] Delattre BM, Van De Ville D, Braunersreuther V, Pellieux C, Hyacinthe JN, Lerch R, et al. High time-resolved cardiac functional imaging using temporal regularization for small animal on a clinical 3 T scanner. IEEE Trans Biomed Eng 2012;59:929–35.
[27] Berry CJ, Thedens DR, Light-McGroary K, Miller JD, Kutschke W, Zimmerman KA, et al. Effects of deep sedation or general anesthesia on cardiac function in mice undergoing cardiovascular magnetic resonance. J Cardiovasc Magn Reson 2009;11:16.
[28] Thomas D, Dumont C, Pickup S, Misselwitz B, Zhou R, Horowitz J, et al. T1-weighted cine FLASH is superior to IR imaging of post-infarction myocardial viability at 4.7 T. J Cardiovasc Magn Reson 2006;8:345–52.
[29] Bohl S, Lygate CA, Barnes H, Medway D, Stork LA, Schulz-Menger J, et al. Advanced methods for quantification of infarct size in mice using three-dimensional high-field late gadolinium enhancement MRI. Am J Physiol Heart Circ Physiol 2009;296:H1200-.
[30] Feiring AJ, Johnson MR, Kioschos JM, Kirchner PT, Marcus ML, White CW. The importance of the determination of the myocardial area at risk in the evaluation of the outcome of acute myocardial infarction in patients. Circulation 1987;75:980–7.
[31] Price AN, Cheung KK, Lim SY, Yellon DM, Hausenloy DJ, Lythgoe MF. Rapid assessment of myocardial infarct size in rodents using multi-slice inversion recovery late gadolinium enhancement CMR at 9.4 T. J Cardiovasc Magn Reson 2011;13:44.
[32] Protti A, Sirker A, Shah AM, Botnar R. Late gadolinium enhancement of acute myocardial infarction in mice at 7 T: cine-FLASH versus inversion recovery. J Magn Reson Imaging 2010;32:878–86.
[33] Skardal K, Rolim NP, Haraldseth O, Goa PE, Thuen M. Late gadolinium enhancement in the assessment of the infarcted mouse heart: a longitudinal comparison with manganese-enhanced MRI. J Magn Reson Imaging 2013;38:1388–94.
[34] Bishop J, Feintuch A, Bock NA, Nieman B, Dazai J, Davidson L, et al. Retrospective gating for mouse cardiac MRI. Magn Reson Med 2006;55:472–7.
[35] Carbone F, Crowe LA, Roth A, Burger F, Lenglet S, Braunersreuther V, et al. Treatment with anti-RANKL antibody reduces infarct size and attenuates dysfunction impacting on neutrophil-mediated injury. J Mol Cell Cardiol 2016;94:82–94.